Chapter 5
Direct and Indirect Effects of Soil Fauna, Fungi and Plants on Greenhouse Gas Fluxes

M. Zaman, K. Kleineidam, L. Bakken, J. Berendt, C. Bracken, K. Butterbach-Bahl, Z. Cai, S. X. Chang, T. Clough, K. Dawar, W. X. Ding, P. Dörsch, M. dos Reis Martins, C. Eckhardt, S. Fiedler, T. Frosch, J. Goopy, C.-M. Görres, A. Gupta, S. Henjes, M. E. G. Hofmann, M. A. Horn, M. M. R. Jahangir, A. Jansen-Willems, K. Lenhart, L. Heng, D. Lewicka-Szczebak, G. Lucic, L. Merbold, J. Mohn, L. Molstad, G. Moser, P. Murphy, A. Sanz-Cobena, M. Šimek, S. Urquiaga, R. Well, N. Wrage-Mönnig, S. Zaman, J. Zhang, and C. Müller

Abstract Soils harbour diverse soil fauna and a wide range of soil microorganisms. These fauna and microorganisms directly contribute to soil greenhouse gas (GHG) fluxes via their respiratory and metabolic activities and indirectly by changing the physical, chemical and biological properties of soils through bioturbation, fragmentation and redistribution of plant residues, defecation, soil aggregate formation,

M. Zaman (✉) · L. Heng
Soil and Water Management & Crop Nutrition (SWMCN) Section, Joint FAO/IAEA Division of Nuclear Techniques in Food and Agriculture, International Atomic Energy Agency (IAEA), Vienna, Austria
e-mail: m.zaman@iaea.org; zamanm_99@yahoo.com

K. Kleineidam · C. Eckhardt · A. Jansen-Willems · G. Moser · C. Müller
Institute of Plant Ecology, Justus Liebig University Giessen, Giessen, Germany

L. Bakken
Norwegian University of Life Sciences (NMBU), Aas, Norway

J. Berendt · S. Fiedler · N. Wrage-Mönnig
University of Rostock, Rostock, Germany

C. Bracken
School of Agriculture and Food Science and Earth Institute, University College Dublin, Dublin, Ireland

K. Butterbach-Bahl
Institute of Meteorology and Climate Research, Atmospheric Environmental Research (IMK-IFU), Karlsruhe Institute of Technology, Karlsruhe, Germany

Z. Cai
School of Geography Sciences, Nanjing Normal University, Jiangsu, China

S. X. Chang
Department of Renewable Resources, University of Alberta, Edmonton, AB T6G 2E3, Canada

herbivory, and grazing on microorganisms and fungi. Based on recent results, the methods and results found in relation to fauna as well as from fungi and plants are presented. The approaches are outlined, and the significance of these hitherto ignored fluxes is discussed.

Keywords Soil fauna · Fungi · Microorganisms · GHG

5.1 Greenhouse Gases from Soil Fauna

5.1.1 Introduction

Soils harbour a diverse group of fauna. Based on their size and the resulting occupied soil space, soil animals can be grouped into microfauna (<200 μm: protists, some nematodes), mesofauna (0.2–2 mm, e.g. nematodes, microarthropods, enchytraeids, molluscs), and macrofauna (>2 mm, e.g. earthworms and other worms, ants, beetles, termites, spiders, molluscs) (Lavelle et al. 2006). These animals directly contribute to soil GHG fluxes via their respiratory and metabolic activities and indirectly by changing the physical, chemical and biological properties of soils through bioturbation, fragmentation and redistribution of plant residues, defecation, soil aggregate

T. Clough
Department of Soil & Physical Sciences, Faculty of Agriculture & Life Sciences,
Lincoln University, Lincoln, New Zealand

K. Dawar
Department of Soil and environmental Sciences, University of Agriculture, Peshawar, Pakistan

W. X. Ding
Institute of Soil Science, Chinese Academy of Sciences, Nanjing, China

P. Dörsch · L. Molstad
Faculty of Environmental Sciences and Natural Resource Management,
Norwegian University of Life Sciences (NMBU), Aas, Norway

T. Frosch
Leibniz Institute of Photonic Technology, Technical University
Darmstadt, Darmstadt, Germany

J. Goopy
International Livestock Research Institute (ILRI), Nairobi, Kenya

C.-M. Görres
Department of Soil Science and Plant Nutrition/Department of Applied Ecology, Hochschule
Geisenheim University, Geisenheim, Germany

A. Gupta
Independent Consultant India, Mumbai, India

S. Henjes · M. A. Horn
Institute of Microbiology, Leibniz University Hannover, Hannover, Germany

formation, herbivory, and grazing on microorganisms and fungi. Additionally, micro-habitats are created that can support greater microbial activity than bulk soil does (Brown et al. 2000; Lubbers et al. 2013). Thus, soil fauna can substantially influence the spatial and temporal variability of GHG fluxes in the field. Additionally, climate, abiotic soil conditions, land management and interactions within the soil food web modify the abundance, activity and vertical distribution of fauna in soils. The magnitude of the effect of soil fauna on soil GHG fluxes remains poorly quantified. Most of our current knowledge comes from laboratory experiments, while field data are scarce, which are often controversial and have been limited to only a few regions and species. Filser et al. (2016) provided the latest review and an extensive literature list on soil fauna and its effects on soil organic matter (SOM) turnover and nutrient cycling. The following sections provide a broad overview of the current knowledge of direct and indirect effects of soil animals on soil GHG fluxes and summarize available field methods for quantifying these effects.

5.1.2 Overview of Fauna on GHG Emissions

5.1.2.1 Carbon Dioxide (CO$_2$)

Spatial clustering of soil fauna can result in an increased spatial variability of soil CO$_2$ emissions due to the creation of CO$_2$ point sources (Ohashi et al. 2007). Positive correlations between soil CO$_2$ emissions and faunal biomass have been observed (Binet et al. 1998), and faunal respiration can contribute between 2 and 40% of total

M. E. G. Hofmann
Picarro B.V., 's-Hertogenbosch, The Netherlands

M. M. R. Jahangir
Department of Soil Science, Bangladesh Agricultural University, Mymensingh, Bangladesh

D. Lewicka-Szczebak
Laboratory of Isotope Geology and Geoecology, Institute of Geological Sciences, University of Wrocław, Wrocław, Poland

G. Lucic
Picarro Inc., Santa Clara, CA, USA

L. Merbold
Mazingira Centre, International Livestock Research Institute (ILRI), Nairobi, Kenya

J. Mohn
Laboratory for Air Pollution & Environmental Technology, Empa Dübendorf, Dübendorf, Switzerland

P. Murphy
Environment & Sustainable Resource Management Section, School of Agriculture & Food Science, and UCD Earth Institute, University College, Dublin, Ireland

A. Sanz-Cobena
Research Center for the Management of Environmental and Agricultural Risks (CEIGRAM), ETSIAAB, Universidad Politécnica de Madrid, Madrid, Spain

soil respiration (Briones et al. 2004; Lubbers et al. 2013). Ignoring these soil CO_2 flux hotspots might result in substantial errors in ecosystem carbon (C) balances (Ohashi et al. 2007). However, indirect effects of the presence of soil fauna on total soil respiration often seem to be more important than direct respiratory contributions.

The most studied soil fauna groups with respect to soil CO_2 fluxes are earthworms, potworms (*Enchytraeids*), termites and beetles. Earthworms are divided into three functional groups based on their feeding and movement patterns in soils. Anecic earthworms live in deeper soil zones where they ingest moderate amounts of mineral soil as well as litter which they drag down from the soil surface into their burrows. Earthworms living and feeding mainly in the rhizosphere are called endogeic. These earthworms ingest substantial amounts of mineral soil. Epigeic earthworms live and feed preferentially in the litter zone above the mineral soil (Horn et al. 2006). Soil properties are altered by its passage through the earthworm gut, and earthworm casts, burrows and middens provide microhabitats for smaller soil animals and microorganisms (Brown et al. 2000; Lubbers et al. 2013). Interactions of functional earthworm groups seem to lead to greater mean soil CO_2 emissions compared to soils where only one functional earthworm group is present (Speratti and Whalen 2008). Increased soil CO_2 emissions through earthworm activity seem to be transient, though in the long-term earthworms might increase C storage in soils through stabilization of SOM in stable micro-aggregates (Lubbers et al. 2013; Six and Paustian 2014).

Earthworm abundances increase and species compositions change when moving from conventional tillage systems to systems with reduced or no tillage (Lubbers et al. 2013). In conventionally tilled fields, enchytraeids seem to be more important for organic matter (OM) mineralization than earthworms (van Vliet et al. 2004). Like earthworms, enchytraeids are burrowing animals that can ingest large amounts of soil, including fungi, bacteria, algae and even dead bodies of larger invertebrates (Briones et al. 2004; van Vliet et al. 2004).

M. Šimek
Institute of Soil Biology, Biology Centre of the Czech Academy of Sciences, and Faculty of Science, University of South Bohemia, České Budějovice, Czech Republic

M. dos Reis Martins · S. Urquiaga
EMBRAPA Agrobiologia Seropédica, Brazilian Agricultural Research Corporation, Seropedica, RJ, Brazil

R. Well
Thünen Institute of Climate-Smart Agriculture, Braunschweig, Germany

S. Zaman
University of Canterbury, Christchurch, New Zealand

J. Zhang
School of Geography, Nanjing Normal University, Nanjing, China

K. Lenhart
Bingen University of Applied Sciences, Berlinstr. 109, Bingen 55411, Germany

Termites are primarily concentrated in tropical grasslands and forests, and based on their nesting habits are classified as mound-building, wood-nesting or subterranean termites (Jamali et al. 2011a). Termite mounds are point sources of CO_2 emissions (Brümmer et al. 2009) which can show large seasonal patterns due to seasonal population dynamics of termites inhabiting the mounds, as well as changes in gas diffusivity of the mound walls (Jamali et al. 2011b, 2013). These patterns are controlled by changes in temperature, moisture, food quantity and quality, as well as the termites' life cycle, and can be highly species-specific (Jamali et al. 2011b). Although total mound CO_2 emissions are mainly comprised of termite respiration, microbial respiration within the mound walls can also be a significant contributor. Suitability of mound walls as habitats for microorganisms depends on properties such as mound bulk density and wall thickness that again can vary widely between termite species (Jamali et al. 2013). Termite CO_2 emissions might be negligible on an ecosystem scale, but uncertainties in CO_2 flux estimates are high (Brümmer et al. 2009; Jamali et al. 2013). These uncertainties are due to a lack of field studies for termites that do not construct mounds, uncertainties in the global estimates of total termite biomass and number of nests, and a lack of process understanding of gaseous exchange between termites and the atmosphere (Jamali et al. 2011a).

In recent years, another group of arthropods has received increasing attention regarding its effects on soil GHG fluxes–dung beetles. On farmland with grazing animals, dung pats are GHG flux hotspots. Dung beetles are important contributors to dung composition and can significantly alter the temporal pattern of CO_2 emissions from dung pats. Dung beetles can either enhance or suppress CO_2 emissions from dung pats based on the species and their feeding behaviours (Penttilä et al. 2013; Piccini et al. 2017).

5.1.2.2 Methane (CH_4)

Soil fauna groups known to emit CH_4 are termites, scarab beetles, millipedes and cockroaches. Emissions have been observed from tropical as well as temperate species, but not from all tested species within a group, and within-group variability is high (Egert et al. 2005; Sustr and Šimek 2009; Brune 2010; Kammann et al. 2017). Methane is produced by methanogenic microorganisms in the insect gut which either live on intestinal surfaces or as endosymbionts inside gut-inhabiting protozoa (Brune 2010). Like termite respiration, termite CH_4 fluxes scale with termite biomass (Jamali et al. 2011b). Methane emitted by termites can significantly affect the CH_4 balance of an ecosystem, offsetting part of the CH_4 sink of the surrounding soil (Jamali et al. 2011a). However, not all CH_4 produced by termites reaches the atmosphere because part of it is oxidized to CO_2 by methanotrophic microorganisms during its diffusive passage through mound walls and the soil surrounding termite nests (Sugimoto et al. 1998; Jamali et al. 2011a, 2013). Termites can also directly enhance CH_4 oxidation as their burrowing activities increase soil diffusivity, and the increasing soil CH_4 concentration supports a larger and more active methanotrophic community (Bender and Conrad 1995). Methane emissions from other soil-dwelling insects have thus

far been regarded as negligible at the ecosystem scale (Egert et al. 2005; Sustr and Šimek 2009). However, recent studies suggest that CH_4 emitted by Scarab beetle larvae have the potential to significantly enhance soil CH_4 oxidation and thus affect the soil CH_4 balance in well-aerated upland soils (Kammann et al. 2017). However, the observations on dung beetles are controversial. Methane emissions from dung pats, especially if they are from grazing dairy cows, can be extremely high, being able to switch a field from a net CH_4 sink to a net CH_4 source. Depending on species, dung beetles have been shown to either drastically reduce or increase dung pat CH_4 fluxes (Penttilä et al. 2013; Piccini et al. 2017). Adult scarab beetles can also be CH_4 sources (Bijnen et al. 1996). Earthworms are generally not considered as CH_4 emitters (Drake et al 2006), but recently, CH_4-emitting earthworms were discovered in Brazil (Schulz et al. 2015).

5.1.2.3   Nitrous Oxide (N_2O)

Earthworms are the only faunal group for which a considerable amount of literature on their effects on soil N_2O fluxes is available (Kuiper et al. 2013). Earthworms themselves as well as their casts and burrow walls can be N_2O emission hotspots, able to increase soil N_2O emissions by more than 40% (Brown et al. 2000; Lubbers et al. 2013). In contrast to CH_4-emitting soil fauna, earthworms do not have a quantitatively significant indigenous microbial biome in their guts. Instead, N_2O emissions are due to the activation of nitrate- and nitrite-reducing bacteria in the ingested material during its gut passage. Conditions favourable for denitrifiers inside the earthworm gut include anoxia, an ample supply of C as well as nitrate and nitrite, a suitable pH, and a high moisture content (Drake and Horn 2006; Horn et al. 2006). Gut passage does not only affect soil denitrifiers, but the overall soil bacterial community composition. This is due to selective digestion of bacteria by the earthworms and the mixing of ingested material with mucus, an aqueous secretion rich in organic molecules (Drake et al. 2006). However, the impact of earthworms on functional bacterial soil communities remains unclear (Chapuis-Lardy et al. 2010).

The impact of earthworms on soil N_2O emissions depends on soil type, environmental conditions, earthworm functional groups and species compositions, but the emissions themselves do not seem to scale with earthworm biomass (Chapuis-Lardy et al. 2010). The impact of earthworms on soil structure, gas diffusion, and N and C availability seems to have a much larger effect on soil N_2O fluxes than direct N_2O emissions from the earthworms (Bertora et al. 2007; Kuiper et al. 2013). Increase in N_2O emissions in the presence of earthworms has only been observed for soils to which crop residues or fertilizers were applied (Chapuis-Lardy et al. 2010; Speratti and Whalen 2008). Earthworms initially speed up residue mineralization and thus increase inorganic N availability. However, as already seen for CO_2 emissions, this seems to be a transient phenomenon and in the long-term earthworm presence may lead to lower N_2O emissions, compared to fields without an abundant earthworm population (Bertora et al. 2007; Chapuis-Lardy et al. 2010). The earthworm effect on N_2O fluxes due to residue incorporation can be partly replaced by ploughing

in agricultural systems (Bertora et al. 2007). Other soil invertebrate fauna can also significantly modify soil N_2O fluxes, both positive and negative, with the effect being dependent on the fauna's ability to modify soil structure and its relative biomass in the soil fauna food web (Kuiper et al. 2013; Penttilä et al. 2013; Piccini et al. 2017). However, for soil fauna groups other than earthworms, studies have mainly focused on N mineralisation, rather than on direct gaseous N fluxes (van Vliet et al. 2004; Kuiper et al. 2013).

5.1.3 Field Methodology

Soil fauna can substantially influence the spatial and temporal variability of GHG fluxes in the field through direct and indirect effects, but it is often logistically or methodologically not possible to quantify them in situ. Nevertheless, a basic knowledge of the local soil fauna can significantly aid the interpretation and upscaling of GHG flux data. Thus, in the planning phase of a GHG flux study, one should consider the following questions:

(i)   What are the key species or functional groups of the soil fauna at the study site and to which degree do they have to be considered in order to reach the aim of the study?
(ii) Are the measurement plots representative for the selected land management types or ecosystems with regard to the soil fauna?
(iii) Do temporal changes in the behaviour of key faunal species or their functional groups have to be considered in the measurement schedule?

There are no standard field methods and measurement protocols available specifically for quantifying soil fauna GHG fluxes since the vast majority of studies have been in the laboratory or in field mesocosms under controlled and simplified conditions. However, all of the measurement methods described in this book can potentially be adapted to quantify soil fauna GHG fluxes in situ, and examples of such adaptations are listed in the following paragraphs.

Measurements of net GHG fluxes with the chamber or eddy covariance method (Chap. 4) include all soil fauna effects at the plot scale regardless of the available knowledge on these animals at a particular field site. Abundances and total biomass of key species and functional groups can be quantified in accompanying soil sampling campaigns. Abundance, weight and vertical distribution in the soil are the easiest parameters to obtain for soil fauna characterization. Greenhouse gas emissions of excavated animals can be directly estimated in the field by incubating them in hermetically sealed vessels, preferably glass vessels. Vessel size (e.g. Exetainers, test tubes, glass jars) and incubation time depend on animal size and expected emission strength (Sustr and Šimek 2009). Figure 5.1 shows a freshly excavated Scarab beetle larva (2.6 g) which was incubated in a 110 ml test tube sealed with a rubber stopper for an hour.

Fig. 5.1 Freshly excavated Scarab beetle incubated in a 110 mL test tube

At the end of the incubation period, 25 ml of gas were extracted from the test tube with a syringe for gas concentration analysis. The GHG emission rates are then calculated from the increase of gas concentrations in the headspace air of the incubation vessel over time. Vessels should be kept in the shade or a cooler to prevent a large temperature increase relative to the soil layer from which the animals were excavated. For incubation times over an hour, wet pieces of paper towel should be added to the vessels to keep the animals from drying out. Each incubation series should include blank measurements (=empty sealed vessels). In some studies, individuals were rinsed with water before incubating them to remove attached soil particles (e.g. Horn et al. 2006). Each vessel should only be used once in the field as earthworms and scarab beetle larvae can defecate during the incubation. Any emissions from the faeces can be determined by sealing the vessel again for at least an hour after the animal has been removed. These incubations can also be performed on soil fauna which is kept in the laboratory under controlled conditions. However, one has to keep in mind that GHG emissions may strongly depend on the available food source and thus, laboratory and field quantifications might not be directly comparable.

Chambers can also be used to measure directly net GHG fluxes by soil fauna clusters like dung pats or termite mounds (Penttilä et al. 2013; Jamali et al. 2011a, b). The flexibility of the chamber and collar design permits it to fit as precisely as possible to the size of the clusters, thus reducing the relative contribution of soil adjacent to the clusters to the measured GHG flux. However, when targeting soil faunal effects

on GHG fluxes with the chamber method, there are two additional considerations which have to be taken into account during construction and installation of permanent collars. First, permanent collar installation can constrain the horizontal movement of soil fauna and, as a result, change their behaviour. Depending on the targeted soil fauna groups, it might not be possible to find a collar insertion depth that adheres to the guidelines for airtight chamber measurements and permits unconstrained soil fauna movement at the same time. Second, the chosen collar material has to be durable enough to withstand any fragmentation attempts by the soil fauna, especially the mandibles of macro-arthropods (e.g. scarab beetle larvae).

Net GHG fluxes at soil fauna clusters may also be quantified using soil gas sampling probes (see Chap. 2, Sect. 2.3.) and the flux gradient technique. Jamali et al. (2013) installed nylon tubes in termite mounds for measuring CO_2 and CH_4 concentrations. Net mound CO_2 and CH_4 fluxes measured with chambers were significantly correlated to the internal mound CO_2 and CH_4 concentrations, respectively. There was also a significant relationship between net mound CH_4 fluxes and internal mound CO_2 concentrations. However, all these relationships were highly species-specific, and using internal mound gas concentrations as a proxy for determining net mound fluxes results in higher uncertainties in the flux estimates compared with direct chamber measurements. Nevertheless, in areas where chamber measurements on termite mounds are not possible, this method can be used with great caution to derive at least rough estimates of net mound CH_4 and CO_2 emissions (Jamali et al. 2013).

Stable isotope methods provide possibilities to measure GHG fluxes in situ without disturbing the soil system and are especially helpful to estimate gross fluxes, such as the contribution of soil fauna. Sugimoto et al. (1998) estimated the proportion of CH_4 oxidized by diffusion through the walls of termite mounds from the difference in $\delta^{13}C$-CH_4 between the CH_4 produced inside the mounds and the CH_4 captured outside during chamber measurements (natural abundance approach). An isotope pool dilution technique developed by von Fischer and Hedin (2002) allows the simultaneous estimation of gross CH_4 production and gross CH_4 oxidation rates in soils. Originally developed for incubating intact soil cores in hermetically sealed vessels, this technique can also be used in combination with chambers (Yang and Silver 2016). Immediately after a chamber is placed airtight onto a collar to start a flux measurement, ^{13}C-CH_4 is injected into the chamber headspace to reach an isotopic enrichment of 2–10 atom % ^{13}C-CH_4. However, headspace CH_4 concentration should remain at the ambient level and not increase by more than 0.1 ppm. The chamber headspace can additionally be labelled with trace amounts of SF_6 (~10 ppb) to quantify diffusional losses of the ^{13}C-CH_4 label from the chamber and then correct the measurement results accordingly. After labelling, the chamber measurement proceeds as usual, taking gas samples either manually with a syringe or automatically with an attached gas analyser (Yang and Silver 2016). Section 5.3 provides a practical example of the analysis of manually collected discrete gas samples with a stable carbon isotope analyser. Gross CH_4 production and gross CH_4 oxidation rates are estimated by fitting equations for the change of the amount of labelled CH_4, the total amount of CH_4, and the isotope ratio over time (von Fischer and Hedin 2002). This technique has

the potential to be used to quantify in situ CH_4 production of soil-dwelling Scarab beetle larvae and other CH_4-emitting macro-arthropods in well-aerated upland soils, although it is yet to be field-tested for this purpose. The various CH_4 production and oxidation processes can also be analysed via a stable isotope tracing model similar to $Ntrace_{Gas}$ described in Chap. 7, Sect. 7.5.7.

Another way to use stable isotopes in soil fauna GHG flux studies is to add ^{13}C and/or ^{15}N labelled plant material to soils. Methane production by scarab beetle larvae in well-aerated upland soils feeding on the residues could be estimated by quantifying the emission of ^{13}C-CH_4 from the soil by using chambers. Measuring ^{15}N-N_2O soil emissions using chambers allows estimation of the plant material contribution to the overall N_2O emissions. Excavated earthworms can be freeze-dried, ball-milled and dried at 60 °C for ^{15}N determination. This information can untangle which of the earthworm species is most active in digesting plant material residues (Giannopoulos et al. 2010).

5.2 Greenhouse Gases from Fungi and Plants

Many experiments focus on the greenhouse gas balance of an ecosystem. Therefore, CH_4, N_2O and CO_2 fluxes from the surface to the atmosphere are measured, either with chamber techniques on a number of plots or–on larger scale–via eddy covariance techniques. With these techniques, the net fluxes of GHG between the ecosystem and the atmosphere can be quantified and the sink or source strength can be determined. Nevertheless, this approach neglects simultaneously occurring production and consumption processes of CH_4 and N_2O plants that are part of the soil–plant–atmosphere continuum (SPAC).

Currently, when investigating greenhouse gas fluxes and emission pathways, the focus lies on microbial-derived greenhouse gas emissions from soils. Recently, it has been shown for a broad range of species that eukaryotic organisms–namely, algae (Scranton and Brewer 1977), fungi (Lenhart et al. 2012), cryptogams (Lenhart et al. 2015), animal cells (Ghyczy et al. 2008) and higher plants (Keppler et al. 2006)— release considerable amounts of CH_4 and N_2O to the atmosphere. From those organisms, only fungi are known to produce N_2O from soil. In addition, fungi can also emit CH_4 (Lenhart et al. 2012). Plants can either be a source of CH_4 (Keppler et al. 2006) and N_2O (Lenhart et al. 2019) themselves, or they can have a "chimney" function, transporting dissolved CH_4 and N_2O via the transpiration stream. Depending on ecosystem and environmental conditions, this will lead to an over- or underestimation of GHG fluxes (Machacova et al. 2016). Lichens and mosses will be of minor importance in most agricultural ecosystems due to their low abundance in managed ecosystems. Nevertheless, depending on cryptogamic biomass and metabolic activity, cryptogam-derived emissions are of relevance in natural ecosystems.
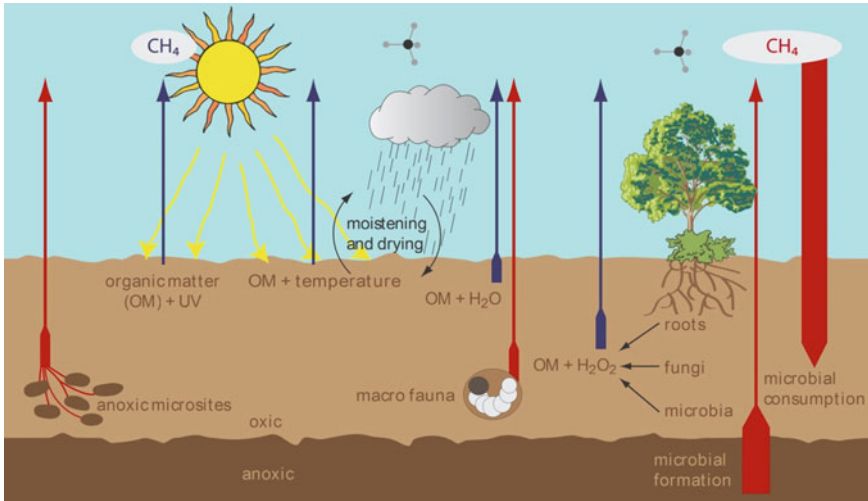
Fig. 5.2 Conceptual scheme of sources and sinks of soil air CH_4 in an aerated soil ecosystem (Jugold et al. 2012). Methane uptake from the atmosphere is the dominant process, biotic CH_4 formation (red arrows) under oxic conditions in plants and fungi, biotic CH_4 formation under anoxic conditions in free-living Archaea and larvae containing methanogenic Archaea in their gut and chemical formation of CH_4 (blue arrows) from soil organic matter are sources of soil air CH_4

5.2.1 Methane (CH_4)

Investigating CH_4 production in aerated soil in the field is difficult because it occurs simultaneously to CH_4 consumption. For aerated ecosystems (e.g. upland soils), CH_4 consumption usually exceeds CH_4 production by several orders of magnitude; thus, it is extremely difficult to detect and quantify small CH_4 production rates. Methane consumption by methanotrophic bacteria is the only biological CH_4 sink of atmospheric CH_4 and causes–due to the arising concentration gradient–flux of CH_4 from the atmosphere into the soil. Besides atmospheric CH_4, which is usually the predominant CH_4 source in aerated soils, several biotic or abiotic sources are known in the plant–soil system (Wang et al. 2013). An overview is given in Fig. 5.2.

Abiotic CH_4 formation from soil organic matter is triggered by solar radiation, temperature and wetting–drying cycles. For a detailed description of abiotic greenhouse gas sources, we refer to Wang et al. (2017). Biotic formation of CH_4 occurs in anoxic microsites and in the gut of soil macrofauna by methanogenic archaea. Plants release CH_4 from roots to soil air and from aboveground biomass directly to the atmosphere. Due to their strong connection via mycorrhiza, it is virtually impossible to distinguish between root- and fungi-derived CH_4 in nature.

Methane formation of methanogenic archaea is restricted to anoxic conditions. Thus, free-living archaea occur in deeper soil layers, water-saturated soils, anoxic microsites or within the gut of soil animals (Hackstein and Stumm 1994). In contrast to *Archaea,* plants and fungi are not restricted to anoxic conditions. Thus, plants

and fungi emit CH_4 in the presence of oxygen (i.e. in upland soils where methane-consuming bacteria occur), although their emission rates are in general much lower than the rates that can be achieved by methanogenic *Archaea* under anoxic conditions. Moreover, the fluxes of CH_4 from these sources (Fig. 5.2) are characterized by a high temporal and spatial variability, depending on the environmental conditions such as temperature, pH, water content, O_2 concentration and substrate availability.

Our knowledge about CH_4 formation from plants and fungi is still rudimentary. Physical damage (Wang et al. 2009; Lenhart et al. 2015), UV-radiation (Bruhn et al. 2014) and inhibition of the cytochrome C oxidase (Wishkerman et al. 2011) leads to an increased formation of CH_4 by plants. The biochemical pathways leading to CH_4 formation in plants and fungi are unknown, although various organic compounds like pectins (Keppler et al. 2008), lignins (Vigano et al. 2008), hydrocarbons (Etiope and Klusman 2002), ascorbic acid (Althoff et al. 2010) and methionine (Lenhart et al. 2015) were identified as a precursor for CH_4 production.

By using isotopic labelling techniques (^{13}C), it is possible to identify the precursors of CH_4. When ^{13}C labelled compounds are added that are metabolized to CH_4, also the ^{13}C label in headspace-CH_4 will be labelled. Moreover, using position-specific components (i.e. compounds where only one atom is ^{13}C labelled), it is even possible to determine a specific atom or functional group of a molecule that is converted to CH_4. One example of position-specific labelling is the amino acid methionine, where only the sulphur bound methyl group of methionine is ^{13}C labelled ($S-^{13}CH_3$). In a laboratory approach, it was shown that sterile cultivated plants are able to convert this methyl group to CH_4 (Lenhart et al. 2015). In a similar experiment where fungi were supplemented with acetate, and where either the carboxy group ($HOO^{13}C-CH_3$) or the methyl group ($HOOC-^{13}CH_3$) was ^{13}C labelled (Fig. 5.3), it was shown that fungi can convert the methyl group of acetate to CH_4.

Fig. 5.3 CH_4 production form ^{13}C labelled acetate in sterile culture of *Pleurotus sapidus* (n = 3) at 25 °C in the dark. $\delta^{13}C$ (**a, b**) and concentration (**c, d**) of headspace CH_4 are presented separately for the control (**a, c**) "medium only" and *P. sapidus* (**b, d**)
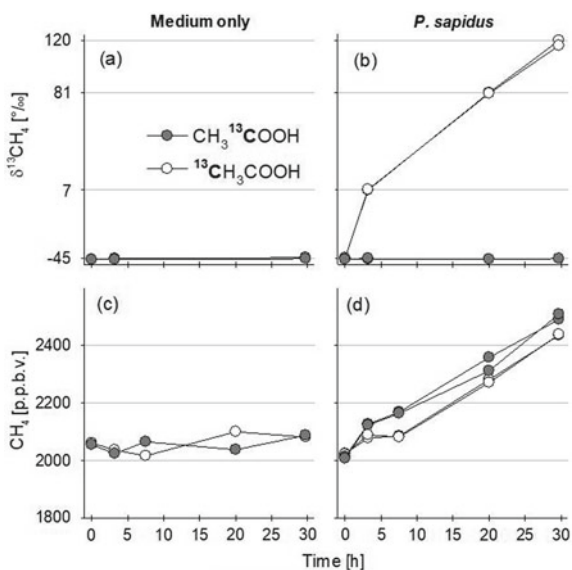
5.2.2 A Laboratory Approach to Study CH_4 Production from Plants and Fungi

Traditional approaches that measure greenhouse gas fluxes from the plant–soil system often measure net fluxes; determination of gross rates is rare. Only one-field study of plant-derived CH_4 exists (Wang et al. 2008). However, to get insights into the complex system of soil air CH_4 sources and sinks occurring in the plant–soil system, we suggest investigating CH_4 production processes under controlled laboratory conditions. We are aware that transfer of laboratory results to the field site is very complex and not always reasonable. On the other hand, with our current knowledge, it is not possible to conduct the following experiments in the field.

To quantify CH_4 formation, a *closed chamber system* (Fig. 5.4) must be used to achieve a sufficient CH_4 enrichment. For open flux chamber systems, the CH_4 (and N_2O) production rates of plants and fungi are probably too low to be detected. This might cause artificial effects, e.g. by affecting gas diffusion (including O_2 availability) in the soil. When measuring CH_4 production in the plant–soil system, methane oxidation by methanotrophic bacteria must be inhibited. This can be achieved with the gaseous inhibitors Difluormethane (DFM, 1 ml l^{-1}) or Acetylene (1 ml l^{-1}). Both substances are reversible inhibitors of the enzyme methane monooxygenase, resulting in a nearly complete inhibition of CH_4 consumption by methanotrophic bacteria.

Fig. 5.4 Example of a closed chamber system that can be used to measure trace gas emissions from organisms–also under sterile conditions. If the lid is equipped with two Festo tube connectors, the flask can be connected to a gas analyser for automated analysis (see Sect. 3.2.2)

5.2.3 Measuring Procedure

Field-fresh soil samples should be sieved (2–6 mm) to increase the diffusivity of the inhibitors in the soil. When collecting soil cores with vegetation (e.g. grassland soil), the efficiency of inhibitors is limited due to the lower diffusivity compared to sieved soil.

Insert the field-fresh sample into an airtight flask or chamber equipped with a septum to collect gas samples or connect it to an online system for trace gas measurements (e.g. Picarro system, Plate 3.10). Add either DFM or Acetylene. To accelerate the diffusion of the inhibitor into the soil, we recommend pressure fluctuations, e.g. by "pumping" air in and out with a syringe (=volume change).

Attention: Those inhibitors often cause interferences with a laser-based system → check before the start of the incubation. It is therefore recommended to collect gas samples and measure the concentration with a GC system.

The time to collect gas samples depends on the concentration change, which in turn depends on the amount of sample, the volume of the flask/chamber and the production rate (mostly temperature dependent). For a temperate grassland soil, we obtained good results with 2.7 l headspace, 300 g samples (soil + vegetation), and 25 °C and 15 h incubation. A pre-experiment is recommended to determine the emission rates of CH_4, N_2O and CO_2 under "normal" conditions before working with inhibitors. Depending on the outcome of this pre-experiment, the system must be adjusted (volume, temperature, amount of sample, sampling time). For all incubations, we add three control flasks where only water was added and no changes in CH_4 concentration over time can be expected. In those flasks, gas concentration should remain constant.

5.3 Measuring Discrete Gas Samples with a Cavity Ring-Down Spectrometer for CO_2 and CH_4 Concentration and Carbon Isotope Analysis

In greenhouse gas flux studies, it is common practice to perform the gas concentration and isotope analysis with a gas chromatograph and mass spectrometer, respectively. Some commercially available optical gas analysers are capable to combine both analyses, thus simplifying sample collection and sample processing for the user. The gas analyses to quantify the concentrations of GHG emissions and the stable isotope compositions as described in Sects. 5.1 and 5.2. were predominantly carried out with an optical analyser. One such analyser is the Picarro G2201-*i* cavity ring-down spectrometer. The Picarro G2201-*i* is a field-deployable analyser capable of simultaneous concentration and $\delta^{13}C$ measurements for both CO_2 and CH_4. It can be directly connected to a chamber for continuous closed-loop measurements or employed for the analysis of discrete gas samples, which is the focus here. The following sections address sample injection modes, carrier gas stream and sample

volume choice, as well as sample processing times specifically for the Picarro G2201-*i*, but large parts of the information are either directly or in a slightly modified version transferable to other commercially available optical gas analysers.

Sample injection mode

An important gas analyser property to consider when designing an experiment is its sample injection mode since this has implications on the maximum number of processible samples and the method of sample storage prior to analysis. The Picarro G2201-*i* has three possible sample injection modes: (a) injecting each sample manually with a syringe directly into the carrier gas stream, (b) injecting each sample manually into a Picarro Small Sample Introduction Module (SSIM) which automatically passes the samples on into the carrier gas stream, or (c) equipping the SSIM with a manifold to completely automate the injection of multiple samples (see Fig. 5.5). For all three discrete injection modes, the basic requirement is the supply of the Picarro G2201-*i* with a continuous carrier gas stream of either dry zero air (i.e. air with <1 ppm CO_2 and CH_4 and <10 ppm H_2O) or dry standard air with ambient trace gas concentrations (Dickinson et al. 2017) at a pressure of ≥ 3 psi (0.2 bar) and <8 psi (~0.5 bar). The slight overpressure at the sample inlet ensures that the analyser can draw in the required ~25 ml min^{-1} into its optical cavity.

An example of a custom-made direct manual sample injection setup has been described by Dickinson et al. (2017). It was tested with different Picarro gas analysers, but the principle of operation can also be transferred to other optical gas analysers. In general, the preferred tubing material for the carrier gas stream line is stainless steel due to its gas tightness and chemical inertness, but PTFE and FEP tubing can also be used, with FEP being the least expensive material. In this case, FEP tubing was equipped with two Luer lock three-way valves. The valve closest to the analyser is the designated sample injection port. Regardless of the sample injection mode, the tubing between the sample injection port and the analyser's sample inlet should be minimized to decrease potential dead volumes, mixing and lag times between sample injection and the actual measurement inside the analyser. The other valve is used for controlling the carrier gas stream. Samples were delivered to the carrier
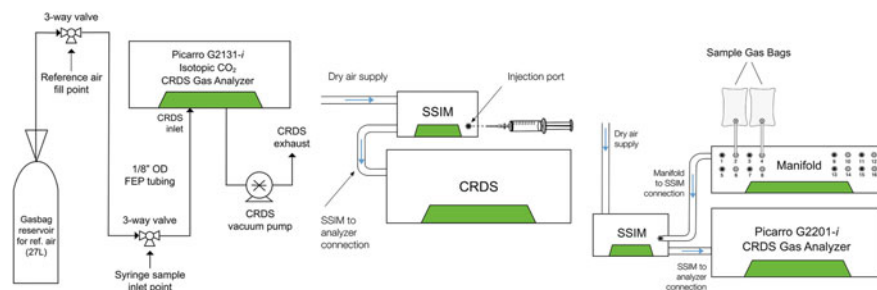

Fig. 5.5 Comparison of different discrete sample injection modes: *left* direct manual injection (figure modified after Dickinson et al. 2017), *center* injection via Small Sample Introduction Module (SSIM) and *right* automated injection of multiple samples via a 16-port-manifold. The manifold allows to attach up to 8 sample bags (every second inlet is capped off for purging cycles)

gas stream with a gastight syringe equipped with a push-button valve and Luer lock fitting. Once the syringe is connected to the sample injection port, the three-way valve is closed manually to stop the carrier gas stream. Then the syringe valve is opened, and the gas sample drawn steadily into the analyser without any further assistance since the analyser operates with a vacuum inside the optical cavity. After complete evacuation of the syringe, the carrier gas stream is manually switched back on. A sample volume of 50 ml was estimated to be the minimum volume for reliable operation of this injection mode. Larger volumes can be administered as well but would require some adjustments in the data processing routine which are described in Dickinson et al. (2017). This custom-made injection setup requires a well-cleaned and silicone-lubricated glass syringe to ensure smooth sample evacuation. Any friction between the plunger and the syringe wall can cause the plunger to jump during sample evacuation which can create small pressure fluctuations inside the analyser's optical cavity and thus increase measurement noise.

Injecting discrete gas samples via the SSIM avoids the problem of possible pressure variations. The SSIM is composed of a 20 ml sample chamber with a sample injection port, a solenoid valve system, an internal pressure sensor and an external vacuum pump. It is inserted into the carrier gas stream line as close as possible to the analyser's sample inlet. The solenoid valve system can shut off the sample cell from the carrier gas stream, but the carrier gas stream into the analyser is never interrupted. At the beginning of a discrete sample measurement, the SSIM is purged with carrier gas and subsequently evacuated several times to remove residues of previous samples. The last pre-measurement step is always a sample chamber evacuation. Injections of discrete sample volumes between 20 and 25 ml can be performed actively with a syringe, or by attaching larger sample containers (e.g. Teflon bags) to the SSIM sample injection port from which samples can be drawn in by the sample chamber vacuum. Once sample injection into the SSIM sample chamber is complete, the sample injection port is closed and the solenoid valve connecting the sample chamber with the carrier gas stream is opened to release the sample into the carrier gas stream. As the pressure in the sample chamber decreases, the outlet valve of the analyser slowly closes to maintain a constant pressure in the cavity. In this way, the flow rate through the cavity is reduced to ensure that the residence time of the sample in the cavity is maximized for a longer peak integration. It is also possible to inject less than 20 ml of gas into the SSIM sample chamber. In that case, the remaining sample chamber volume is filled up with carrier gas prior to releasing the sample to the analyser, resulting in sample dilution. This process is later in this case study referred to as automatic zero air dilution. When working in the dilution mode, one has to make sure that the CO_2 and/or CH_4 concentrations are within the dynamic range of the analyser. The standard specification range for the G2201-i is 380–2000 ppm for CO_2 and 1.8–1000 ppm for CH_4 (unless the analyser was upgraded for low and/or high CO_2 concentration measurements).

To automate discrete sample injection, the SSIM can be equipped with a 16-port manifold. The 16-port manifold is a rotary valve that allows to attach up to 8 discrete samples, while the other 8 ports must be closed off so that they can be used for purging between measurements to reduce memory effects due to sample carry-overs. Also,

when attaching the manifold to the SSIM, it is important to keep the tubing as short as possible to reduce dead volume effects which might degrade the accuracy for concentration measurements. The sequence of sample and standard measurements can be defined in the SSIM control software (referred to as 'Coordinator' software) also allowing for repeated sample injection. After defining the measurement sequence and other measurement parameters, the SSIM performs a purge and pump step and then asks the user to attach all sample containers to the manifold keeping the valves to the container closed. The Coordinator software then starts another purge and pump cycle for all selected input ports, and once completed, the user has to manually open all sample container valves before the actual unattended sample measurement starts. The duration of a single measurement takes 12 or 8 min in the standard or fast measurement mode, respectively (Fig. 5.5).

Effect of carrier gas and sample volume on the measurement result

The Picarro G2201-*i* continuously measures gas concentrations and $\delta^{13}C$ in its optical cavity at a rate of approximately three to five seconds depending on whether one focuses only on the stable carbon isotopes of one gas species or the simultaneous quantification of both $\delta^{13}C$-CO_2 and $\delta^{13}C$-CH_4. The carrier gas stream provides a baseline measurement on which discrete sample measurements are superimposed as peaks. Choosing dry standard air instead of zero air as carrier gas is foremost an economical choice, but it has important implications for the data processing. Adding zero air to a discrete gas sample dilutes it resulting in lower CO_2 and CH_4 concentrations. However, the isotopic signature of the sample remains unchanged since no additional ^{12}C and ^{13}C are added to the sample. There are three possible reasons for diluting discrete gas samples: (a) it was not possible to collect sufficiently large gas sample volumes during an experiment, (b) CO_2 and/or CH_4 concentrations in the samples are too high and exceed the analyser's operational range, or (c) the samples contain contaminants (e.g. ammonia, hydrogen sulphide, ethylene) in high enough concentrations to negatively affect the spectroscopic measurements. When the Picarro G2201-*i* is coupled with the SSIM, the analyser's software automatically calculates the isotopic signature for each discrete gas sample regardless of whether it has been diluted with zero air in the SSIM or not, and no further data processing by the user is required. However, there is a limit to sample dilution. If the absolute concentrations of ^{12}C and ^{13}C in the sample approach the lower end of the analyser's operational range, instrument noise can increase to a degree that a reliable estimate of the isotopic signature becomes impossible.

Under certain conditions, the Picarro G2201-*i* is also able to provide reliable CO_2 and CH_4 concentration measurements (Picarro Application Note AN038). As previously mentioned, zero air addition to a discrete gas sample dilutes its CO_2 and CH_4 concentrations and ultimately biases the measurement result towards the carrier gas. Biases can also be introduced by sample carry-overs. Sample carry-overs are significantly reduced in the SSIM by the purging and evacuation cycles taking place immediately prior to sample injection. To physically limit zero air dilution of the sample, it is important to minimize the path length between the SSIM injection port and the sample, e.g. by using a septum port, and to inject at least 20 ml of gas into

the SSIM sample chamber. If less sample is injected, a bias in the concentration data is unavoidable and has to be corrected by post-processing the data.

Dickinson et al. (2017) have developed data post-processing routines to correct for biases in the analyser's output data, both for the concentration and the δ^{13}C values. Post-processing of the δ^{13}C-CO_2 and δ^{13}C-CH_4 is required when dry standard air is used as carrier gas since it already contains CO_2 and CH_4 at ambient levels with a specific stable carbon isotopic signature. Another important point to consider when opting for dry air as carrier gas is that its CO_2 and CH_4 concentrations and their isotopic signatures have to be significantly different from the expected values in the discrete gas samples because otherwise no unambiguous peak identification in the analyser's continuous data output can be achieved.

Sample processing time

The processing time for a single discrete gas sample depends on the injection mode, the sample volume and required analyser precision. For the direct injection of 50 ml samples into the carrier gas stream, the sample-to-sample time is ~5 min. Half of this time is needed for complete sample evacuation from the syringe. If one likes to use this injection mode with sample volumes >50 ml, sample-to-sample time will increase accordingly (Dickinson et al. 2017). For the combination of the Picarro G2201-*i* with the SSIM, the user has the possibility to choose between a standard and a fast measurement mode, which have a sample-to-sample time of 15 and 10 min, respectively. This includes 3 min for the purge and evacuation cycle to clean the SSIM and the analyser between samples. The actual measurement times for the δ^{13}C and concentration values are 4 min and 9 min for the fast and standard mode, respectively. The analyser's software reports the discrete sample measurement results as averages with their respective standard deviations for these time intervals. Longer measurement time per sample increases measurement precision, but significantly reduces the amount of processible samples per day. The sample-to-sample time is independent of the gas sample volume injected into the SSIM sample cell since the SSIM adds carrier gas to the sample cell if less than 20 ml have been injected. As a result, the SSIM always releases the same gas sample volume into the carrier gas stream. However, if a user is not accustomed yet to manually injecting discrete samples into the SSIM sample cell or if there is a problem during the injection, significant time can be lost during this step and sample-to-sample times can increase up to 20 min. Daily sample throughput can be maximized by automating the entire sample injection process, i.e. equipping the SSIM with a programmable manifold. This does not decrease sample-to-sample times, but samples can also be processed during laboratory off-hours since no personnel has to be present for the sample injection process. For the calculation of the total number of processible samples per day, one does not only have to take into account the number of discrete gas samples obtained from an experiment, but also allocate time for instrument warm-up periods and instrument maintenance as well as the regular analysis of gas standards.

A practical example of discrete gas sample measurements with a Picarro G2201-i

This example demonstrates step-by-step workflow for discrete gas sample measurements with a Picarro G2201-*i* equipped with an SSIM. The focus of this

example is solely on the physical handling of the gas samples and the analyser setup. Post-processing of the measurement data to account for biases will not be discussed but we refer to the considerations described by Dickinson et al. (2017). The gas samples were from a field study using chambers to measure soil CO_2 and CH_4 fluxes. 45 ml gas samples were taken from the chambers and stored in 20 ml screw-capped glass vials which were sealed with pierceable grey chlorobutyl rubber septa. The overpressure serves as protection against sample contamination during transport in case of minor leakages, and to ensure the extraction of ~20 ml of gas from the vials for injection into the SSIM to minimize sample dilution.

Figure 5.6 shows an example of how a sample measurement plan for the analysis of discrete gas samples with a Picarro G2201-i can look like. The first row identifies the experiment and the day on which the gas samples were obtained. The second row lists the names of the files in which the measurement data is stored on the analyser. As soon as the analyser is operational after being switched on, it automatically starts recording all data it collects regardless of whether the user will later use the data for analysis or not. These continuous data are stored in dat files at a sampling rate of approximately three to five seconds depending on the chosen measurement mode. In this example, the dat file name includes the date and the instrument time at which it was generated. To operate the SSIM, the CRDS coordinator software has to be installed on the analyser and launched, as well as a software monitoring the pressure inside the SSIM sample cell. The coordinator software automatically detects the peaks and integrates the signals to provide average $\delta^{13}C$ and gas concentration values and their uncertainties for each discrete sample injected via the SSIM. The discrete data are stored in csv files, and the file names also include the date and the instrument time at which it was generated as well as the abbreviation SSIM. When using the concentration data, e.g. for the calculation of soil chamber fluxes, one has to make sure to use the dry concentration values, not the uncorrected wet concentration values as this could lead to flux underestimation.

Sampling campaign:		Mesocosms	27.09.2017					
File ID:	CFIDS2102-20180124-112533Z-DataLog_User.dat				CFIDS2102-SSIM-20180124-103635.csv			
Vial ID	Sample ID	SSIM Run Num	ml injected	SSIM pressure injec.	SSIM pressure dilut.	Injection time	Comments	
zero air	Continuously measuring zero air with the Picarro Analyzer via the SSIM, start time: 10:40							
zero air		1	0.0	7.8	978.2	11:30		
lab air		2	20.0	926.8	983.6	11:40		
lab air		3	15.0	702.6	981.7	11:50		
lab air		4	10.0	472.1	982.5	12:00		
lab air		5	5.0	250.7	980.9	12:10		
lab air		6	20.0	921.1	979.5	12:20		
245	Mesocosm_2b_t1	7	19.0	943.5	984.4	12:30		
246	Mesocosm_2b_t2	8	19.5	977.6	981.6	12:40		
249	Mesocosm_2b_t3	9	19.0	968.7	985.9	12:50		
247	Mesocosm_2b_t4	10	18.5	923.8	987.8	13:00		
177	Mesocosm_7b_t2	11	19.0	959.3	984.5	13:11		
248	Mesocosm_8b_t0	12	19.5	981.7	982.9	13:21		
250	Mesocosm_8b_t1	13	18.5	946.0	986.9	13:31		
251	Mesocosm_8b_t2	14	19.0	958.8	985.1	13:41		
252	Mesocosm_8b_t3	15	18.5	936.4	988.6	13:51		
253	Mesocosm_8b_t4	16	17.5	891.9	989.7	14:01		
lab air		17	20.0	925.8	985.9	14:11		
zero air		18	0.0	8.0	988.7	14:21		

Fig. 5.6 Example of a measurement plan for a Picarro G2201-i equipped with an SSIM

The measurement plan in Fig. 5.6 contains columns for sample descriptions (vial and sample id), a running number which is taken from the csv file (SSIM Run Num), the injected sample volume (ml injected), the pressure inside the SSIM sample cell after sample injection (SSIM pressure injec.) and after automatic zero air dilution (SSIM pressure dilut.), the time at which each sample was injected into the SSIM (injection time), and comments. The measurement schedule consists of three different phases–a start-up phase, a leak testing and calibration phase, and the actual measurement phase. The start-up phase includes all the necessary steps to get the analyser ready for discrete sample injection. If the analyser is not running yet, but still has to be switched on, it needs at least 45 min to warm up and achieve the necessary vacuum in its optical cavity, after which it should run for about two more hours just measuring room air for laser stabilization. This is to ensure the best possible analyser performance. The next step is to connect the carrier gas stream to the SSIM and the SSIM to the analyser (Fig. 5.7). Before conducting any discrete sample measurements, the analyser should be purged with the carrier gas for about an hour to ensure the absence of memory effects. A well-established carrier gas reading is also essential for any required data post-processing due to memory effects and data biases (Dickinson et al. 2017). These preparatory steps can also be conducted the day before the actual discrete measurements. However, if the carrier gas is zero air, it
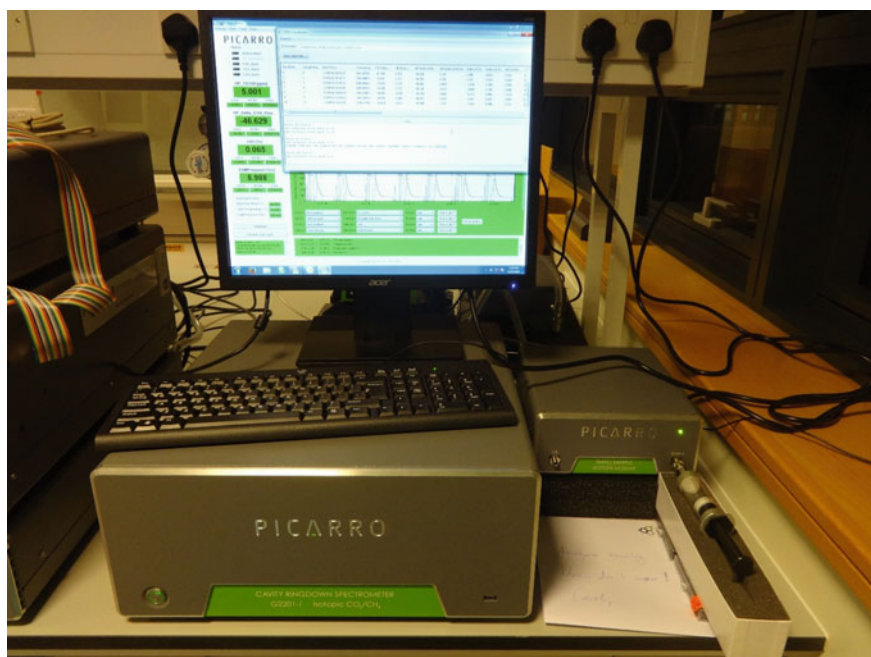

Fig. 5.7 A Picarro G2201-*i* (large box) equipped with an SSIM (small box to the right) during measurements. A syringe containing a discrete sample can be seen attached to the SSIM sample injection port

is not recommended to have the analyser measure the gas stream for several hours as the uninterrupted absence of CO_2 and CH_4 can cause the analyser to drift and offset the analyser's calibration.

Once the analyser is ready for the injection of discrete gas samples, it is very important to perform leak tests and any calibration checks deemed necessary before measuring unknown samples. The most common location for leakages is the sample injection port. In this example, the SSIM injection port was equipped with a so-called septum injector nut with ¼" GC septum (VICI International, Schenkon, Switzerland). The septum used was a 6-mm-thick EC grade, high-temperature silicone septum (Trajan Scientific Europe Ltd, Milton Keynes, United Kingdom). A septum injector nut provides the shortest possible injection pathway from the sample to the SSIM sample cell. It is screwed onto the SSIM injection port, but it is very important not to overtighten the nut. Nut overtightening can significantly compress the septum, thus reducing the septum's flexibility and resealing capability, ultimately resulting in leakage. Additionally, a tightly compressed septum is more difficult to pierce with a needle.

To check the overall system's gas tightness, one should monitor the water concentration and the SSIM pressure. When the dry carrier gas stream is connected to the analyser, the water concentration should drastically drop below 10 ppm and then very slowly continue to decrease throughout the measurement day. The slow continuous decrease is due to the fact that it takes a significant amount of time to purge an analyser completely of all moisture as water vapour attached to the tubing walls will only slowly detach and enter the carrier gas stream. To specifically check the gas tightness of the SSIM, one should first perform a discrete sample injection without actually injecting a sample (Fig. 5.6, SSIM Run Num 1). The normal injection routine for the SSIM consists of six steps: (1) The SSIM coordinator prompts the user to attach a syringe with a vacuum-proof valve to the sample injection port with the syringe valve closed. (2) The sample cell including the tubing to the injection port (and thus the syringe needle) is purged with carrier gas and subsequently evacuated to remove any gas residues. (3) The user is prompted to open the syringe valve, and the sample is sucked into the sample chamber by the vacuum as indicated by a slowly inward moving plunger. As the vacuum in the sample cell is diminished by the inflowing sample, the plunger movement will slow down, and the user has to press in the plunger completely to finish the sample injection. Once the sample has been injected, the syringe can be removed. (4) The sample cell is filled up with carrier gas if necessary (=automatic zero air dilution). (5) The gas in the sample cell is released into the carrier gas stream.(6) The SSIM is purged with carrier gas and evacuated several times to prepare it for the next sample. When no sample is injected during step 3, the pressure in the sample cell should remain stable at ~0 Torr (Fig. 5.6, SSIM pressure injec.). If the injection port is not gastight, the pressure in the sample cell will slowly increase. This test should be regularly repeated since the septum wears down with time and then has to be changed. If no sample is injected, the sample cell is filled with ~20 ml of carrier gas in step 4. The total amount depends on the actual pressure of the carrier gas stream which is depicted by "SSIM pressure dilute" in Fig. 5.5. The user's manual reading of this value from the analyser screen will vary a

bit because this is only a short pressure spike in the sample cell before the sample is released to the analyser. However, the exact value can be retrieved later from the dat file if necessary. Apart from the stable vacuum during step 3, the discrete carrier gas sample measurement should have a water vapour concentration only slightly above the reading of the continuous carrier gas stream if the injection port is gastight.

Apart from leakage checks, the SSIM pressure can be used to estimate the volume for a gas sample if the user does not know it. The relationship between the gas volume and the pressure in the SSIM sample cell is theoretically perfectly linear. The first six measurements in Fig. 5.5 were all injections of known gas sample volumes which were used to construct a simple linear regression model. The resulting equation was

$$SSIM\,pressure\,injec.\,[Torr] = 45.576 Torr/mL * Volume_{injected}[mL] + 15.130 Torr$$

with $R^2 = 1.000$. If the user is not able to establish this linear relationship with an R^2 value of 1, this is also indicative of leakages in the system. This equation was used to later calculate the gas sample volumes for the unknown samples (Fig. 5.6, SSIM Run Num 7–16). These samples were extracted from the 20-ml screw-capped glass vials. The syringe used was a 25-ml 1025 SL Hamilton SampleLock Syringe for 22 gauge needles. To retrieve a discrete sample from a glass vial, the syringe needle was inserted into the vial and the syringe plunger pulled out all the way to the 25 ml mark. The plunger was held in this position for about five seconds to assure that a pressure equilibrium was reached between the vial and the syringe as the air needed some time to flow through the needle. Then the syringe valve was closed, and the plunger could be released. When transferring the sample from the vial to the syringe, the sample gas will equilibrate between these two volumes and only a part of the actual sample gas can be used for analysis, the remainder stays behind in the vial. Thus, as mentioned before, it is mandatory to have an overpressure in the vial of at least the volume which one wishes to inject into the analyser. After the sample was secured in the syringe, the plunger was gently pressed into the syringe until it met a slight resistance and then released again. The mark at which the plunger finally stopped was an indicator of the sample volume retrieved from the vial, albeit a very rough one. This value was noted down in the "ml injected" column; however, the precise SSIM pressure reading during sample injection was later used to derive a better sample volume estimate as described above.

At the end, a small remark regarding the syringe needle. We recommend the usage of side port needles to prevent septum coring. Septum coring means that the needle detaches a piece of silicone from the septum while piercing it. Usually, this silicone piece gets stuck inside the needle completely blocking it. A sure sign for coring is that the syringe plunger does not start to move when the syringe is subjected to the SSIM sample cell vacuum. However, needle blockage also means that no sample can be lost when coring occurs. One can simply close the syringe valve, remove the syringe, clean the needle, and repeat the injection. Needles which are open at the tip are much more prone to coring than side port needles. Side port needles are more expensive than other needle types; however, in the long run, frequent septum coring

requires the septum in the injector nut to be changed more often and one also loses valuable measurement time.

References

Althoff F, Jugold A, Keppler F (2010) Methane formation by oxidation of ascorbic acid using iron minerals and hydrogen peroxide. Chemosphere 80:286–292

Bender M, Conrad R (1995) Effect of CH_4 concentrations and soil conditions on the induction of CH_4 oxidation activity. Soil Biol Biochem 27:1517–1527

Bertora C, van Vliet PCJ, Hummelink EWJ, van Groenigen JW (2007) Do earthworms increase N_2O emissions in ploughed grassland? Soil Biol Biochem 39:632–640

Bijnen FGC, Harren FJM, Hackstein JHP, Reuss J (1996) Intracavity CO laser photoacoustic trace gas detection: cyclic CH_4, H_2O and CO_2 emission by cockroaches and scarab beetles. Appl Opt 35:5357–5368

Binet F, Fayolle L, Pussard M (1998) Significance of earthworms in stimulating soil microbial activity. Biol fertil Soil 27:79–84

Briones MJI, Poskitt J, Ostle N (2004) Influence of warming and enchytraeid activities on soil CO_2 and CH_4 fluxes. Soil Biol Biochem 36:1851–1859

Brown GG, Barois I, Lavelle P (2000) Regulation of soil organic matter dynamics and microbial activity in the drilosphere and the role of interactions with other edaphic functional domains. Eur J Soil Biol 36:177–198

Bruhn D, Mikkelsen TN, Rolsted MMM, Egsgaard H, Ambus P (2014) Leaf surface wax is a source of plant methane formation under UV radiation and in the presence of oxygen. Plant Biol 16:512–516

Brümmer C, Papen H, Wassmann R, Brüggemann N (2009) Fluxes of CH_4 and CO_2 from soil and termite mounds in south Sudanian savannah of Burkina Faso (West Africa). Glob Biogeoch Cyl 23: GB1001

Brune A (2010) Methanogens in the digestive tract of termites. In: Hackstein JHP (ed) (Endo)symbiotic Methanogenic Archaea (Microbiology Monographs). Springer, Berlin, pp 81−100

Chapuis-Lardy L, Brauman A, Bernard L, Pablo AL, Toucet J, Mano MJ, Weber L, Brunet D, Razafimbelo T, Chotte JL, Blanchart E (2010) Effect of the endogeic earthworm *Pontoscolex corethrurus* on the microbial structure and activity related to CO_2 and N_2O fluxes from a tropical soil (Madagascar). Appl Soil Ecol 45:201–208

Dickinson D, Bodé S, Boeckx P (2017) System for $\delta^{13}C–CO_2$ and xCO_2 analysis of discrete gas samples by cavity ring-down spectroscopy. Atmosph Meas Tech 10:4507–4519

Drake HL, Horn MA (2006) Earthworms as a transient heaven for terrestrial denitrifying microbes: a review. Engl Life Sci 6:261–265

Drake HL, Schramm A, Horn MA (2006) Earthworm gut microbial biomes: Their importance to soil microorganisms, denitrification, and the terrestrial production of the greenhouse gas N_2O. In: König H, Varma A (eds): Intestinal microorganisms of termites and other invertebrates. Soil Biology, vol 6. Springer, Berlin, Heidelberg

Egert M, Stingl U, Dyhrberg Bruun L, Pommerenke B, Brune A, Friedrich MW (2005) Structure and topology of microbial communities in the major gut compartments of Melolontha melolontha larvae (Coleoptera: Scarabaeidae). Appl Environ Microbiol 71:4556–4566

Etiope G, Klusman RW (2002) Geologic emissions of methane to the atmosphere. Chemosph 49:777–789

Filser J, Faber JH, Tiunov AV, Brussaard L, Frouz J, De Deyn G, Uvarov AV, Berg MP, Lavelle P, Loreau M, Wall DH, Querner P, Eijsackers H, Jimenez JJ (2016) Soil fauna: key to new carbon models. Soil 2:565–582

Ghyczy M, Torday C, Kaszaki J, Szabo A, Czobel M, Boros M (2008) Hypoxia-induced generation of methane in mitochondria and eukaryotic cells—an alternative approach to methanogenesis. Cell Physiol Biochem 21:251–258

Giannopoulos G, Pulleman MM, van Groenigen JW (2010) Interactions between residue placement and earthworm ecological strategy affect aggregate turnover and N_2O dynamics in agricultural soil. Soil Biol Biochem 42:618–625

Hackstein JH, Stumm CK (1994) Methane production in terrestrial arthropods. PNAS 91(12):5441–5445

Horn MA, Mertel R, Gehre M, Kästner M, Drake HL (2006) In vivo emission of dinitrogen by earthworms via denitrifying bacteria in the gut. Appl Environ Microbiol 72:1013–1018

Jamali H, Livesley SJ, Dawes TZ, Hutley LB, Arndt SK (2011a) Termite mound emissions of CH_4 and CO_2 are primarily determined by seasonal changes in termite biomass and behaviour. Oecologia 167:525–534

Jamali H, Livesley SJ, Grover SP, Dawes TZ, Hutley LB, Cook GD, Arndt SK (2011b) The importance of termites to the CH_4 balance of a tropical savanna woodland of Northern Australia. Ecosyst 14:698–709

Jamali H, Livesley SJ, Hutley LB, Fest B, Arndt SK (2013) The relationships between termite mound CH_4/CO_2 emissions and internal concentration ratios are species specific. Biogeosci 10:2229–2240

Jugold A, Althoff F, Hurkuck M, Greule M, Lenhart K, Lelieveld J, Keppler F (2012) Non-microbial methane formation in oxic soils. Biogeosci 9(12):5291–5301

Kammann C, Ratering S, Görres CM, Guillet C, Müller C (2017) Stimulation of methane oxidation by CH_4-emitting rose chafer larvae in well-aerated grassland soil. Biol fertil Soil 53:491–499

Keppler F, Hamilton JTG, Brass M, Röckmann T (2006) Methane emissions from terrestrial plants under aerobic emissions. Nature 439:187–191

Keppler F et al (2008) Methoxyl groups of plant pectin as a precursor of atmospheric methane: evidence from deuterium labelling studies. New Phytol 178:808–814

Kuiper I, de Deyn GB, Thakur MP, van Groenigen JW (2013) Soil invertebrate fauna affect N_2O emissions from soil. Glob Chang Biol 19:2814–2825

Lavelle P, Decaens T, Aubert M, Barot S, Blouin M, Bureau F, Margerie P, Mora P, Rossi JP (2006) Soil invertebrates and ecosystem services. Eur J Soil Biol 42:3–15

Lenhart K, Bunge M, Ratering S, Neu TR, Schuttmann I, GreuleM Kammann C, Schnell S, Müller C, Zorn H et al (2012) Evidence for methane production by saprotrophic fungi. Nat Commun 3:1046

Lenhart K, Weber B, Elbert W, Steinkamp J, Clough T, Crutzen P, Pöschl U, Keppler F (2015) Nitrous oxide and methane emissions from cryptogamic covers. Glob Chang Biol 21:3889–3900

Lenhart K, Behrendt T, Greiner S, Steinkamp J, Well R, Giesemann A, Keppler F (2019) Nitrous oxide effluxes from plants as a potentially important source to the atmosphere. New Phytol 221:1398–1408

Lubbers IM, van Groenigen KJ, Fonte SJ, Six J, Brussaard L, van Groenigen JW (2013) Greenhouse-gas emissions from soils increased by earthworms. Nat Clim Chang 3:187–194

Machacova K, Back J, Vanhatalo A, Halmeenmaki E, Kolari P, Mammarella I, Pumpanen J, Acosta M, Urban O, Pihlatie M (2016) Pinus sylvestris as a missing source of nitrous oxide and methane in boreal forest. Sci Rep 6:23410

Ohashi M, Kume T, Yamane S, Suzuki M (2007) Hot spots of soil respiration in an Asian tropical rainforest. Geophys Res Lett 34:L08705

Penttilä A, Slade EM, Simojoki A, Riutta T, Minkkinen K, Roslin T (2013) Quantifying beetle-mediated effects on gas fluxes from dung pats. PLoS ONE 8:e71454

Picarro Inc (2018) Application Note AN038. Measuring small volume gas concentrations with the SSIM, pp 1–3

Piccini I, Arnieri F, Caprio E, Nervo B, Pelissetti S, Palestrini C, Roslin T, Rolando A (2017) Greenhouse gas emissions from dung pats vary with dung beetle species and with assemblage composition. PLoS ONE 12:e0178077

Schulz K, Hunger S, Brown GG, Tsai SM, Cerri CC, Conrad R, Drake HL (2015) Methanogenic food web in the gut contents of methane-emitting earthworm *Eudrilus eugeniae* from Brazil. ISME J 9:1778–1792

Scranton MI, Brewer PG (1977) Occurrence of methane in the near-surface waters of the western subtropical North Atlantic. Deep Sea Res 24:127–138

Six J, Paustian K (2014) Aggregate-associated soil organic matter as an ecosystem property and a measurement tool. Soil Biol Biochem 68:4–9

Speratti AB, Whalen JK (2008) Carbon dioxide and nitrous oxide fluxes from soil as influenced by anecic and endogeic earthworms. Appl Soil Ecol 38:27–33

Sugimoto A, Inoue T, Kirtibutr N, Abe T (1998) Methane oxidation by termite mounds estimated by the carbon isotopic composition of methane. Glob Biogeoch Cyl 12:595–605

Sustr V, Šimek M (2009) Methane release from millipedes and other soil invertebrates in Central Europe. Soil Biol Biochem 41:1684–1688

van Vliet PCJ, Beare MH, Coleman DC, Hendrix PF (2004) Effects of enchytraeids (Annelida: Oligochaeta) on soil carbon and nitrogen dynamics in laboratory incubations. Appl Soil Ecol 25:147–160

Vigano I et al (2008) Effect of UV radiation and temperature on the emission of methane from plant biomass and structural components. Biogeosci 5:937–947

von Fischer JC, Hedin LO (2002) Separating methane production and consumption with a field-based isotope pool dilution technique. Glob Biogeoch Cyl 16:10

Wang ZP, Han XG, Wang GG, Song Y, Gulledge J (2008) Aerobic methane emission from plants in the Inner Mongolia steppe. Environ Sci Tech 42:62–68

Wang S et al (2009) Methane emissions by plant communities in an alpine meadow on the Qinghai-Tibetan Plateau: a new experimental study of alpine meadows and oat pasture. Biol Lett 5:535–538

Wang ZP, Chang SX, Chen H, Han XG (2013) Widespread non-microbial methane production by organic compounds and the impact of environmental stresses. Earth Sci Rev 127:193–202

Wang ZP, Han SJ, Li HL, Deng FD, Zheng YH, Liu HF, Han XG (2017) Methane production explained largely by water content in the heartwood of living trees in upland forests. J Geophys Res-Biogeo 122:2479–2489

Wishkerman A et al (2011) Enhanced formation of methane in plant cell cultures by inhibition of cytochrome c oxidase. Plant, Cell Environ 34:457–464

Yang WH, Silver WL (2016) Net soil-atmosphere fluxes mask patterns in gross production and consumption of nitrous oxide and methane in a managed ecosystem. Biogeosci 13:1705–1715

The opinions expressed in this chapter are those of the author(s) and do not necessarily reflect the views of the International Atomic Energy Agency, its Board of Directors, or the countries they represent.